

Enhancement of velocity field estimation by Common Scatter Point gathers

Hassan Khaniani and John C. Bancroft

ABSTRACT

The pre-stack Kirchhoff migration approach is based on a model of subsurface scatter points that act as secondary sources. According to Huygens principle, in the case that scatter points lie on a reflecting interface, and if they are close to each other, superposition of their responses produces a coherent reflection event. Equivalent Offset Migration (EOM) is based on the pre-stack Kirchhoff method that maps the energies of scatter points onto intermediate Common Scatter Point (CSP) gathers that, after successfully applying a Normal Move Out (NMO) correction will create the migrated image. Since the data in the CSP gathers are sorted along hyperbolic paths, it serves as a useful tool for velocity analysis.

In this paper, we studied the behaviour of CSP gathers in areas that have strong lateral velocity variation. In this situation, we showed that the traveltimes response in equivalent offset domain is a tilted hyperbola that is asymmetric around the vertical axis. The reason for the tilt is due to approximate linear time shifts that depend on the dip angle and the degree of velocity variation along the dipping interface. This effect reduces the resolution and accuracy of velocity field picking in the semblance plots. We used three methodologies that can remedy this situation. These methods include producing two sided CSP gathers and analysing the left and right sided gathers separately, estimating the tilt value using a least squares fitting approach, and defining a Linear Time Shifted Hyperbolic Radon (LTSHR) transform.

INTRODUCTION

Let S be a source and G be a receiver, and let R be the scatter point. In the general case where the velocity inside the Earth is arbitrary, the Double Square Root (DSR) equation serves as a starting point for total traveltime $t(S, G)$ approximation from S to R and from R to G (Yilmaz, 2001)

$$t(S, G) = t_{SR} + t_{RG} = \left[\frac{t_0^2}{4} + \frac{|X-h|^2}{v_m^2} \right]^{1/2} + \left[\frac{t_0^2}{4} + \frac{|X+h|^2}{v_m^2} \right]^{1/2}. \quad (1)$$

In this approximation, t_0 is zero offset two-way travel time, h is the half source/receiver offset, X is the distance from source/receiver midpoint to lateral coordination of scatter point and v_m is the migration velocity.

The DSR equation could be simplified into many different hyperbolic forms (Fowler, 1997). Bancroft et al. (1998) has introduced EOM as a pre-stack time migration method that transformed the DSR domain from (X, h, t_0) to the equivalent offset (h_e) domain using the formula:

$$h_e = \text{sgn}(X) \left[X^2 + h^2 - \left(\frac{2Xh}{tv_m} \right)^2 \right]^{1/2} \quad (2)$$

Hence, the new coordinate h_e is chosen so that the travelttime equation becomes the equation of a hyperbola, independent of the location of sources and receivers (Bancroft et al., 1998, Margrave et al., 2001)

$$t(S, G) = \left[t_0^2 + \left(\frac{2h_e}{v_m} \right)^2 \right]^{1/2} \quad (3)$$

From these possibilities, as shown in Figure 1, the equivalent offset method is the only formulation that maps and sums data along the DSR isochrones to all CSP gathers. Therefore, the data do not experience time shifting before NMO process (Bancroft, 1994, Margrave et al., 2001). An alternate view is that the formation of a CSP gather is based on the distances from the source and receivers to the CSP location and not on the source/receiver offset, thus leading to a more natural method of processing Bancroft (1994). Once the CSP gather is formulated, all that remains to complete the pre-stack is a NMO correction, scaling and stacking.

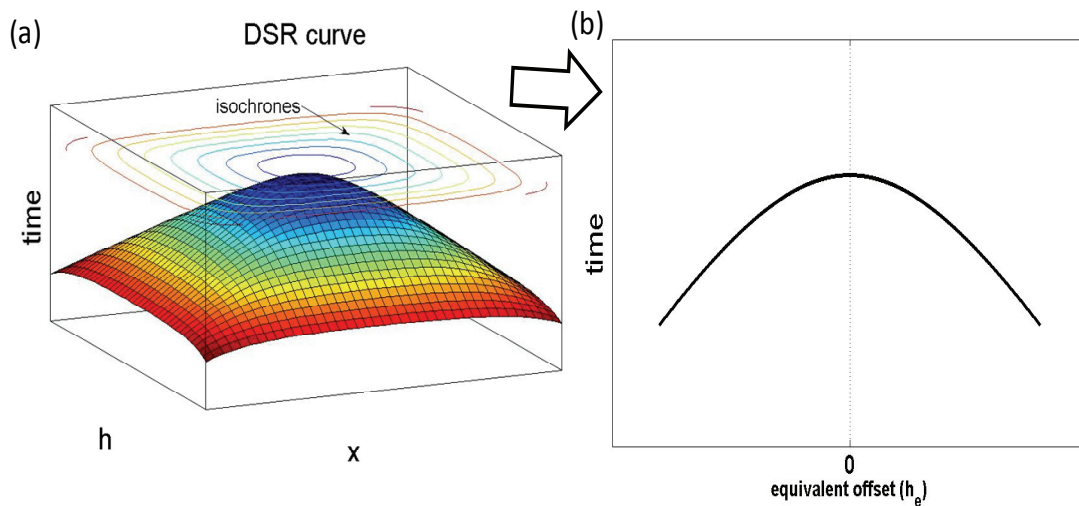


FIG. 1. Kinematics of formation of CSP gathers from a constant velocity model containing one scatter point. Possible energies from (a) input traces of DSR curve is summed along isochrones to produce (b) the hyperbolic event in equivalent offset domain.

The process of mapping the wavefield in data space to an equivalent space can be considered as an efficient algorithm for velocity estimation. The time and velocity dependent cross term $(2Xh/tv_m)^2$ in equation (2) requires a velocity estimate to form CSP gathers. The effect of this cross term is minimal when X or h is small, or when the traveltimes are large. “This allows a significant portion of the input energy to be summed

into a CSP gather using only the asymptotic equivalent offset, which provides stability to the CSP process when the velocities are unknown” (Bancroft et al., 1998).

In an accompanying paper, we described the possibility of modeling the CSP response from any scatter point using ray tracing. We showed that even in complex structures the CSP gather is a generalized gather that is possible to be modeled if an appropriate traveltimes response from the scatter point is available.

In this work, we first showed that traveltimes response of scatter points beneath the dipping interface experiences an additional linear time shifts. This is because the rays bend as a consequence of velocity change. In this situation the CSP data are mapped in asymmetric hyperbolae. This causes inaccuracy in velocity analysis, since the right and left sided CSP gathers demonstrate different velocity in semblance plots. Hence, because of the time shifts, the resolution of semblance plots is reduced. As an example we studied Marmousi data sets and then removed this effect by two practical approaches.

PRINCIPLES OF LINEAR TIME SHIFTS

Figure 2a shows a simple model with a horizontal interface that separates two layers with two different velocities. Wavefront propagation from one scatter point at $4000m$ from left edge of this model and depth of $2500m$ is simulated by connecting isochrones of traced rays. To simply show the possible response from a scatter point (R) beneath the dipping interface with dip angle of β , Figure 2a is rotated by β degrees counter clockwise as depicted in Figure 2b. The new recording surface records the wavefront that is not symmetric around the green axis. This affects the traveltimes response to be no longer symmetric. From the geometrical analysis of the isosceles triangle of Figure 2b the added time (Δt) along the recording surface (x) is approximated as

$$\Delta t = \frac{2 \sin\left(\frac{\beta}{2}\right)}{v_{ave}(x, t)} x, \quad (4)$$

with $v_{ave}(x, t)$ being the average velocity and β is the geological dip. Consequently, the one-way traveltimes response can be approximated by adding a linear time shift to the normal hyperbola.

Using numerical analysis of the DSR equation (1) in equivalent offset domain, as shown in Figure 3a, the traveltimes in equivalent offset domain from a scatter point within a model with a dipping interface is simulated. In Figure 3b, the recorded traveltimes response from the scatter point (blue dotted curve) and the corresponding normal symmetric hyperbola (red curve) are compared. Figure 3c shows the difference between two curves. The difference curve indicates an approximate linear time shift at small equivalent offsets as

$$t_{\text{tilted}} \approx t_{\text{normal}} + \alpha h_e, \quad (5)$$

where, t_{normal} is the traveltime of a normal hyperbola if the diffraction rays pass through a horizontal interface (as shown in Figure 3a) and t_{tilted} is the real traveltime in the form of the tilted hyperbola. The parameter α is the tilt coefficient that affects the velocity inversion.

IMPLEMENTATIONS FOR VELOCITY INVERSIONS IN MARMOUSI EXPERIENCE

In this section, we demonstrated the concept of linear time shifts in Marmousi data sets which consists of 240 shots that spaced at $25m$. The spread has 96 receivers separated by $25m$ at an offset of $200m$ from the shot (Versteeg, 1994).

As shown in Figure 4, the Marmousi complex model contains dipping interfaces with lateral velocity variations. As an example, we analysed the CSP gather at the $x = 3200m$ coordinate of the model. In Figure 4 the rays and wavefront behaviour from a scatter point response at the depths of $1500m$ and $2400m$ are simulated. The ray tracing traveltimes are converted to the equivalent offset domain using equations (2) and (3). As shown in Figure 5, the modeled equivalent offset domain traveltimes (modeled CSP gather) shows a reasonable fit with the real CSP gather obtained from synthetic data.

In Figure 6, the CSP gather and its semblance plot are shown. In the semblance plot, the black and red ellipse show the focussing of the energies from left and right sides of the CSP gather respectively. Note that the resolution of the semblance plot is reduced due to the effect of a linear time shift on the left and right side of CSP gather. In practice, because of different amplitude scaling on both sides of CSP gathers, their semblance values on the final semblance plot can be different.

As a rule of thumb, the velocities inside each layer are easily computed from the average values provided by the semblance analysis of the left and right sided CSP gathers. Figure 7 shows the left sided CSP gather and its semblance plot. As an example, around the time of 2.1 seconds, the semblance shows the velocity of $2480m/s$. Similarly, the right sided CSP gather and its semblance plots are shown in Figure 8 and the picked velocity at the same time is $2700m/s$. So the average value of $2590m/s$ for migration velocity is approximated. Note that the RMS velocity v_{RMS} of the model estimated by the Dix equation is $2470m/s$. The difference between the picked average velocity and RMS velocity is due to the fact that equation for the RMS velocity is based on flat and horizontal layers that have negligible lateral velocity variations.

This approach is fast and computationally inexpensive, but the accuracy is low. To resolve the accuracy problems, two more methodologies are suggested.

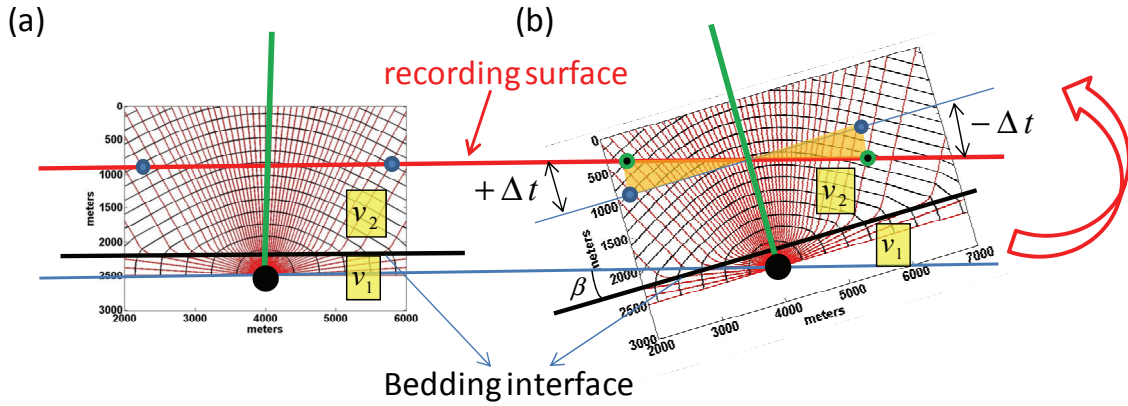


FIG. 2. Principles of linear time shift (Δt). Traveltime response of a diffraction rays passing through (a) a horizontal interface model that has two velocities v_1 and v_2 is rotated to resemble (b) a dipping interface response

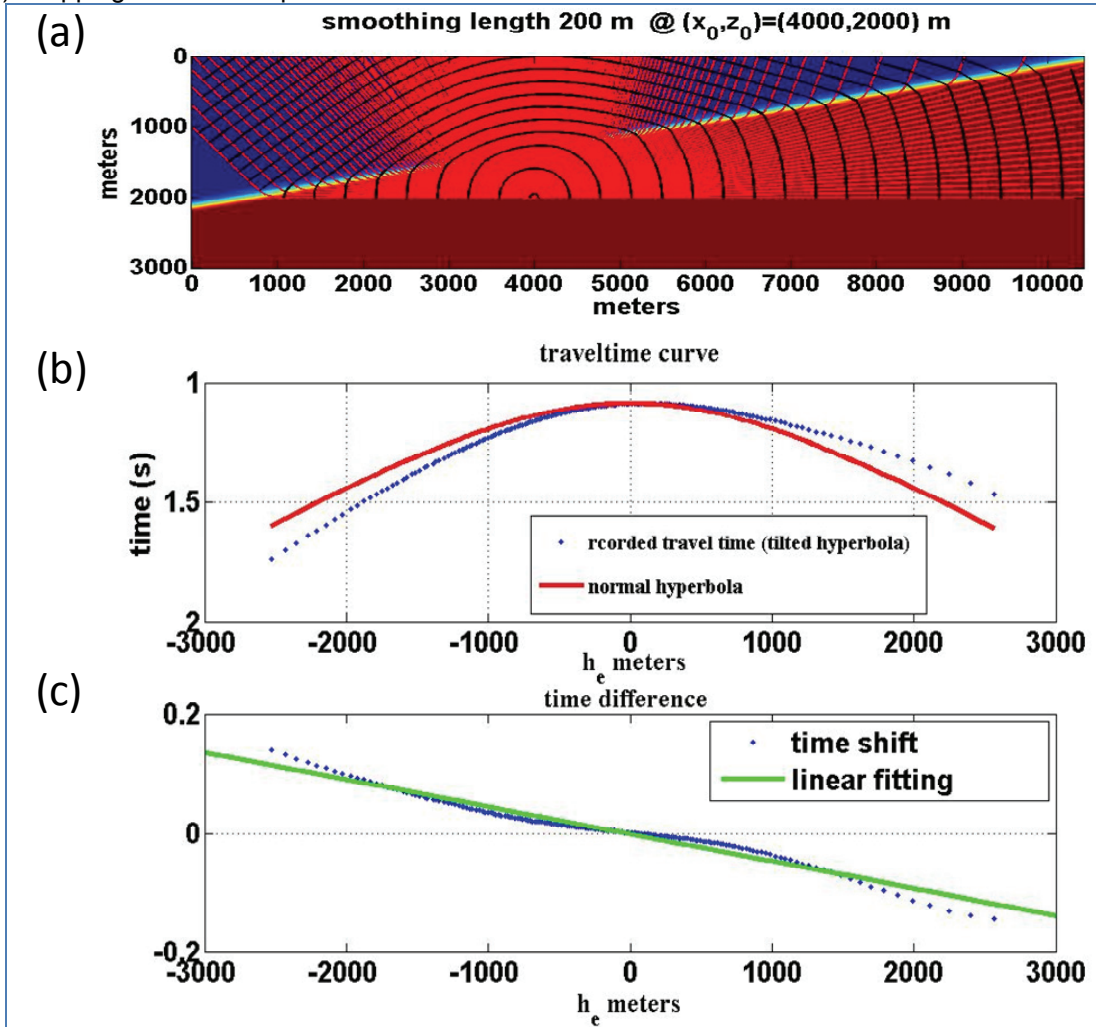


FIG. 3. Traveltime simulation (a) rays and wavefront construction of a diffraction of a scatter point under a simple dipping interface (b) recoded traveltime in equivalent offset domain (blue) with normal hyperbola (red) (c) the time shifts.

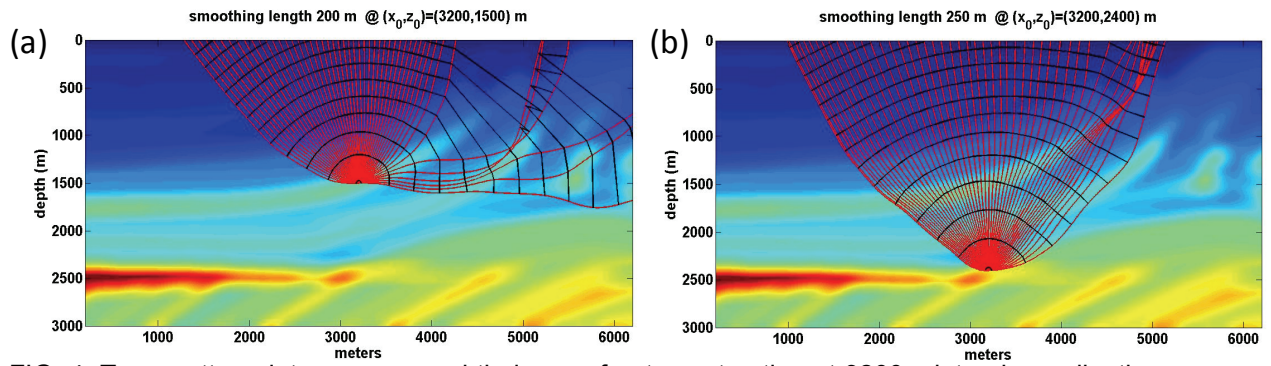


FIG. 4. Two scatterpoint response and their wavefront construction at 3200m lateral coordination of Marmousi model at depth of (a) 1500m and (b) 2400m .

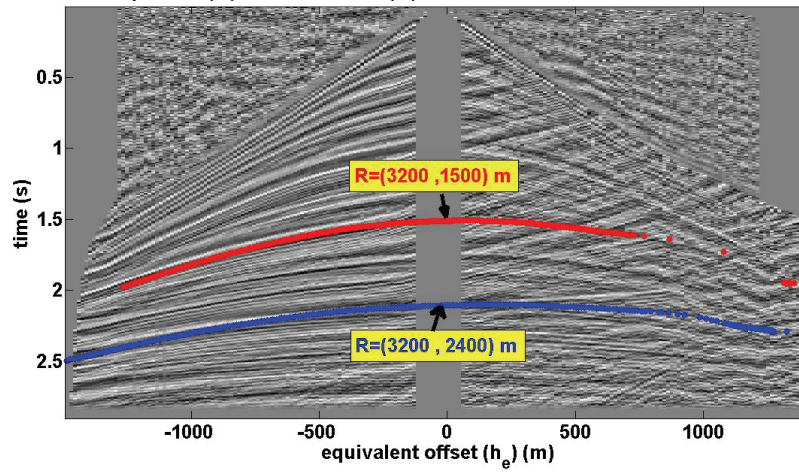


FIG. 5. Comparison of modeled scatter point responses shown in Figure 4 in equivalent offset domain and CSP gather.

METHOD (A): APPLICATION OF HYPERBOLAE LEAST SQUARE FITTING

If the parameters of hyperbolic equation of CSP data are determined then it is possible to find its other properties, such as tilt and its principle axis. Then we are able to rotate its principle axis to the vertical and determine its velocity.

Given n points of the CSP events (i.e., (h_e, t)), the equation of the hyperbola can be formed as the product of a row and column vector such that the point coordinates yield a small residual r_i called the algebraic distance as

$$\begin{bmatrix} x_1^2 & x_1 y_1 & y_1^2 & x_1 & y_1 & 1 \\ \vdots & \vdots & \vdots & \vdots & \vdots & \vdots \\ \vdots & \vdots & \vdots & \vdots & \vdots & \vdots \\ \vdots & \vdots & \vdots & \vdots & \vdots & \vdots \\ \vdots & \vdots & \vdots & \vdots & \vdots & \vdots \\ x_n^2 & x_n y_n & y_n^2 & x_n & y_n & 1 \end{bmatrix} \begin{bmatrix} a \\ b \\ c \\ d \\ e \\ f \end{bmatrix} = \begin{bmatrix} r_i \\ \vdots \\ \vdots \\ \vdots \\ \vdots \\ r_n \end{bmatrix}, \quad (6)$$

where, x_i and y_i are equivalent offsets and times in our problem (i.e., $x_i = 2h_e$, $y_i = t_i$).

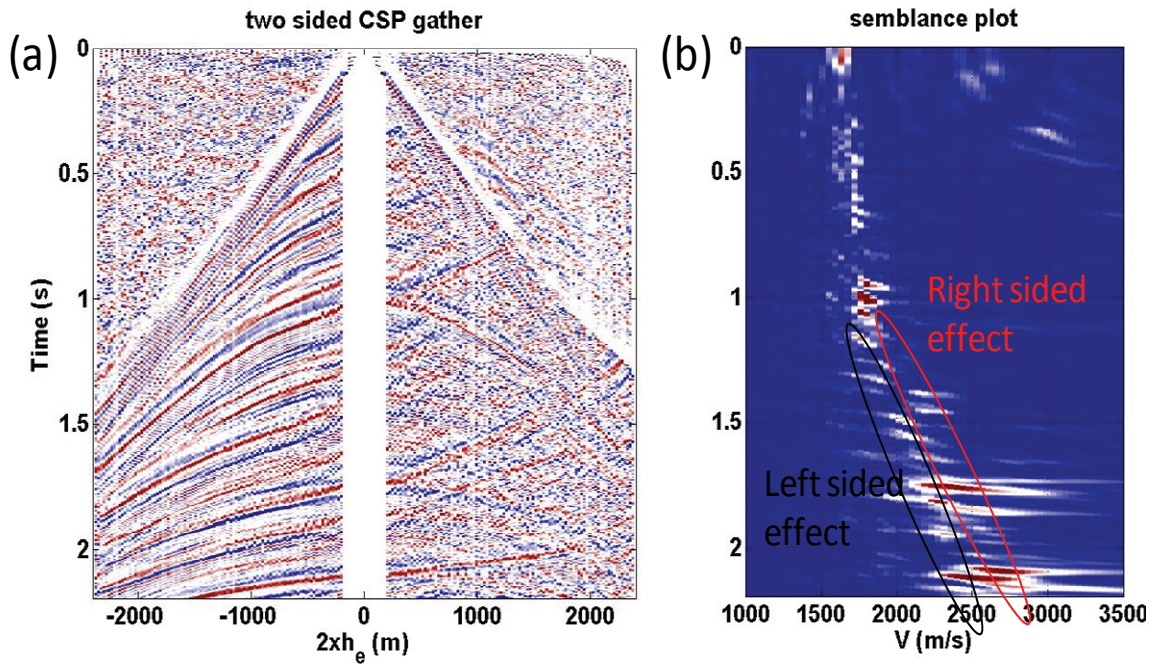


FIG. 6. Velocity analysis at CSP gather at 3200m from left edge of Marmousi model (a) a two sided CSP gather (b) semblance plot and two velocity trends

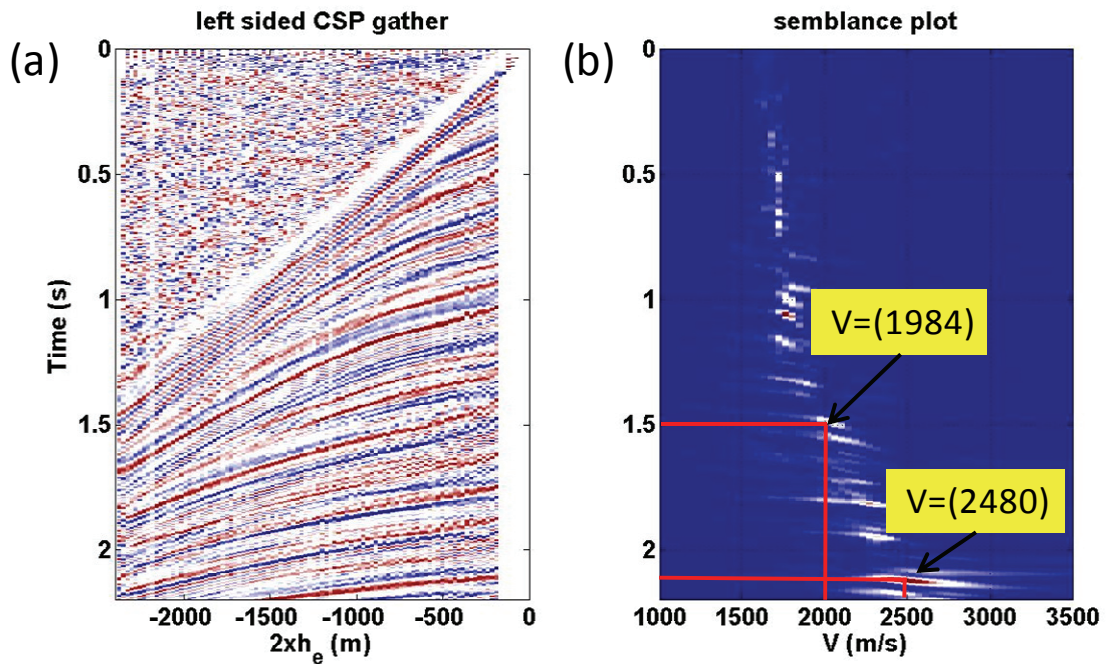


FIG. 7. Velocity analysis at CSP gather at 3200m from left edge of Marmousi model (a) a left sided CSP gather (b) semblance plot

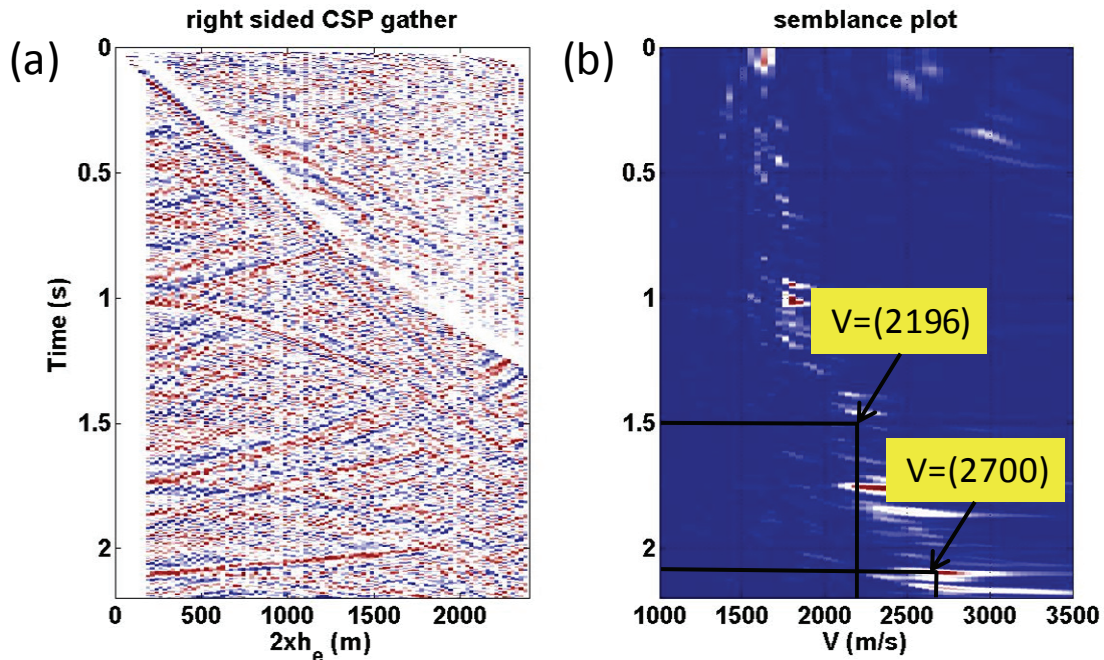


FIG. 8. Velocity analysis at CSP gather at 3200m from left edge of Marmousi model (a) a right sided CSP gather (b) semblance plot

The purpose of least squares fitting is to determine the values of the coefficients (i.e., the coefficient vector, which minimize the sum of the square of the errors). The least squares fitting problem under a constraint could be solved using generalized eigenvectors λ (Leary, 2004). In this study, we followed the method proposed by Leary (Leary, 2004) that finds the equation of non-symmetric hyperbolae by a least squares fitting approach.

In Figures 9-10, the modeled traveltimes of two events at zero offset time of $t_0 = 1.5s$ and $t_0 = 2.1s$ are analysed. The blue curve in traveltimes curves show the original time versus equivalent offset domain. The green curve is the normal hyperbola after removing the tilt from blue curve by least squares. To determine the true migration velocity, we fit the computed normal hyperbola with an ideal hyperbola. Comparing original times with the normal hyperbola, we see the expected linear time shift in the traveltimes difference curves. For two events shown in Figure 4 (i.e., the red and the blue curves in Figure 5), the tilt coefficients for $t_0 = 1.5s$ and $t_0 = 2.1s$ are found to be $\alpha = -2.23 \times 10^{-5}$ and $\alpha = -2.3 \times 10^{-5}$, respectively. This is an accurate approach and the efficiency of this approach needs picking scattered events properly.

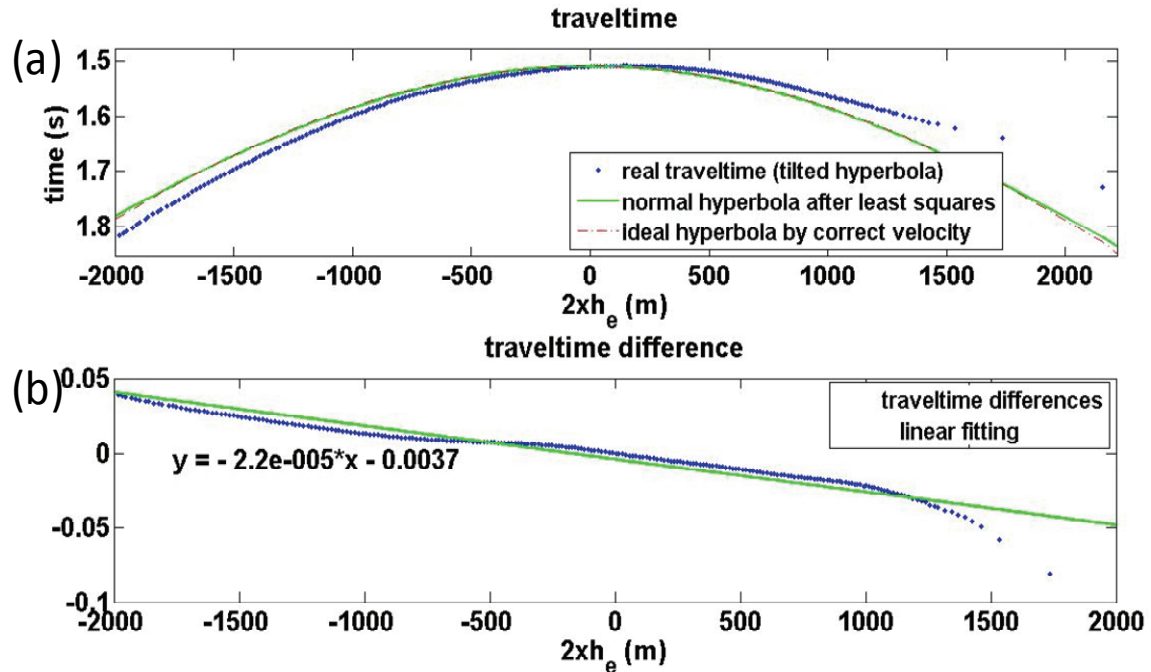


FIG. 9. Modeled traveltimes analysis of CSP gather formed at $3200m$ from left edge of Marmousi model (a) comparisons of traveltimes of $t=1.5s$ (red curve in Figure 5) with its normal hyperbola (b) the linear time shifts

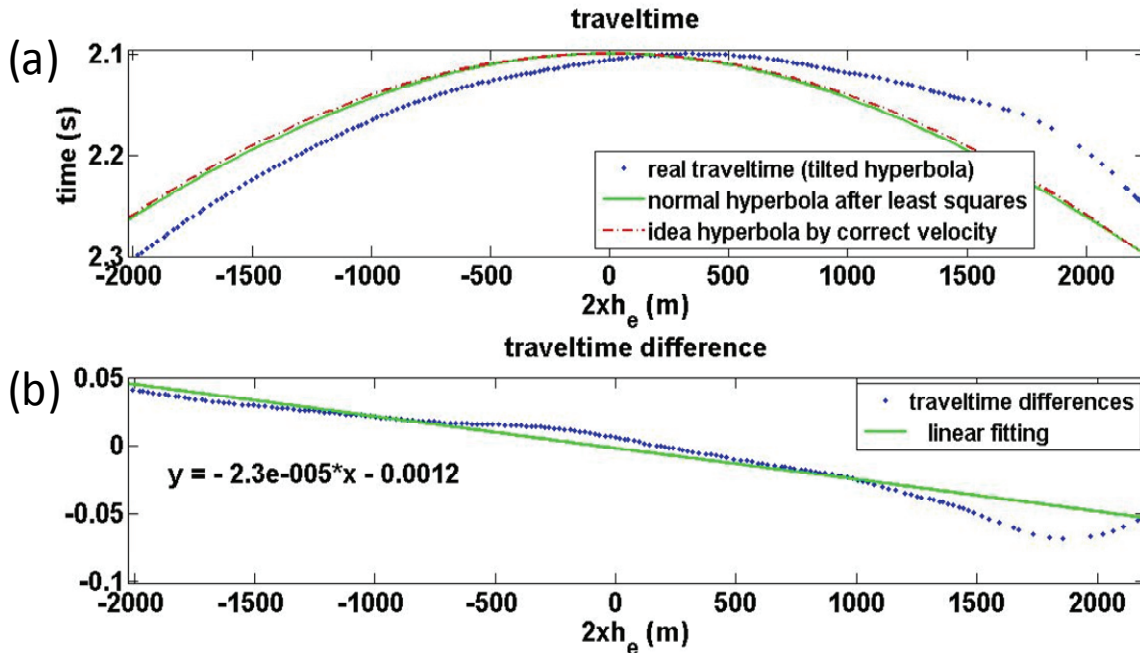


FIG. 10. Modeled traveltimes analysis of CSP gather formed at $3200m$ from left edge of Marmousi model (a) comparisons of traveltimes of $t=2.1s$ (blue curve in Figure 5) with its normal hyperbola (b) the linear time shifts

METHOD (B): LINEAR TIME SHIFTED HYPERBOLIC RADON TRANSFORM

Let d represent a seismic signal in a CSP gather. In order to map the hyperbolic event to a focused point in the hyperbolic Radon domain, we introduce a LTSHR transform that

counts the traveltimes path defined by equation (5). Therefore, the stacking path in Radon formula is defined as:

$$u(t_0, q, \alpha) = \int \int_{\alpha, h_e} d \left(t = \left[t_0^2 + \left(\frac{2h_e}{q} \right)^2 \right]^{1/2} + \alpha h_e, h_e \right) dh_e d\alpha, \quad (7)$$

with t being the two-way travel-time and q the migration velocity. The algorithm for creation of the LTSHR domain (as well as the corresponding semblance cube) is similar to the hyperbolic Radon transform, with an additional loop introduced for different tilt coefficients α . Dimensions of the new transform cube depends of the number of time sample, the number of velocity increments, and the number of coefficients (i.e., $nt_0 \times nq \times n\alpha$).

The semblance cube of the CSP gather is shown in Figure 11. The left face of the cube represents the regular semblance plot (i.e., $\alpha = 0$). From the left face to the right, semblance plot achieved by increasing the tilt coefficient, α . As expected for an optimum α , unfocusing effects due to the linear time shift (tilt in the hyperbola) are removed. This can be seen clearly in two semblance time slices for $t_0 = 1.5s$ and $t_0 = 2.1s$ in Figure 12. The black curve in the semblance cube (Figure 11) indicates the picked optimum values of α at every interval. Finally, for velocity picking, semblance values of all optimum α were selected. In Figure 12, we compared the regular semblance plot with the modified semblance plot obtained by the optimum α . Comparing the focusing of semblance values shows that the clarity for velocity picking has increased in this approach. As shown in Table 1, the picked velocity in this approach is close to the least squares fitting approach that was computed as a reference from ray tracing over the velocity model.

Table 1. Comparison of two picked velocities with least square fitting approach

Method	$t = 1.5s$	$t = 2.1s$	Errors with reference to least square fitting of modeled traveltimes
Picked velocity from left sided CSP	1984	2480	3.16%
Picked velocity from right sided CSP	2196	2700	6.28%
Taking average values of left sided and right sided CSP gather	2090	2590	2.03%
Hyperbolic Least square fitting	2105	2505	0
LTSHR transform	2150	2520	1.59%

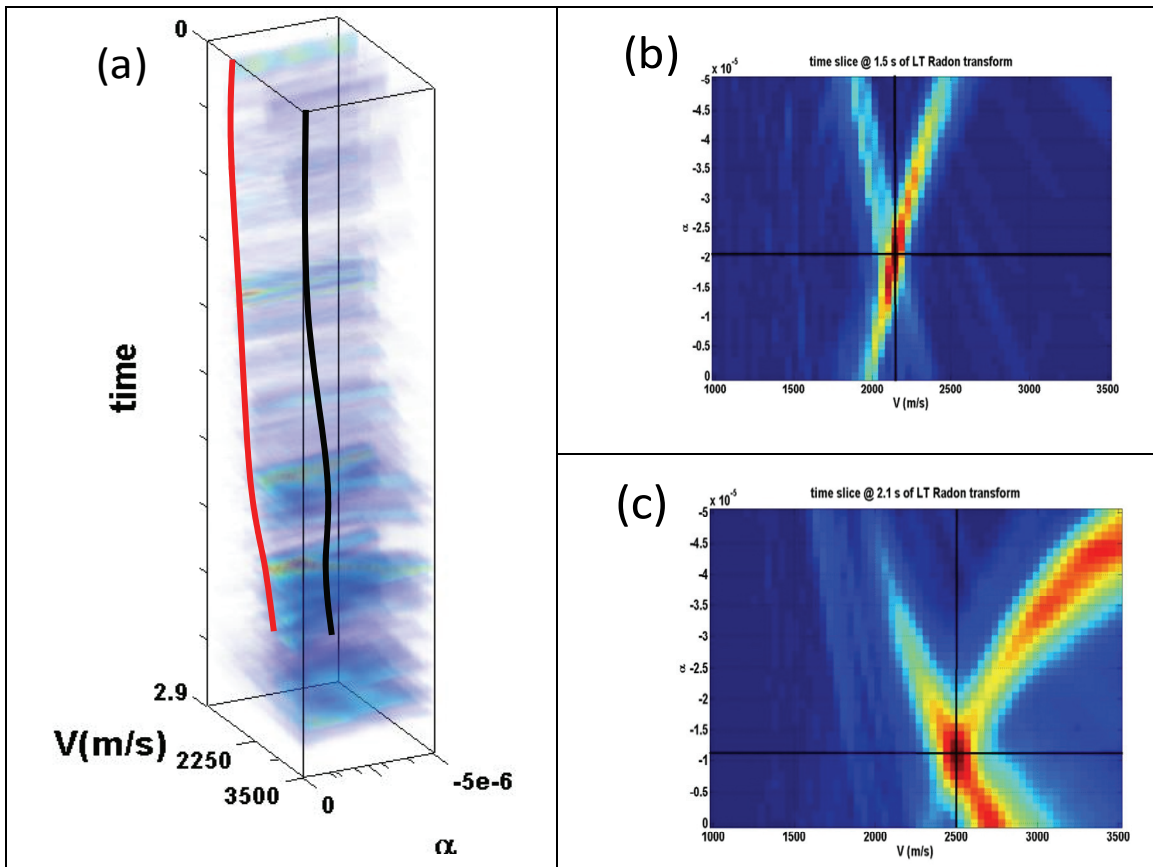


FIG. 11. (a) The Semblance cube computed based on LTSHR transform. Note that the cube has the dimensions of $726 \times 60 \times 40$ (b) The time slices of semblance cube for $t_0 = 1.5s$ that shows the optimum focusing energies occurs by $\alpha = -2.1 \times 10^{-5}$. (c) The time slice for $t_0 = 2.1s$ shows that the optimum focusing energy occurs by $\alpha = -1.3 \times 10^{-5}$.

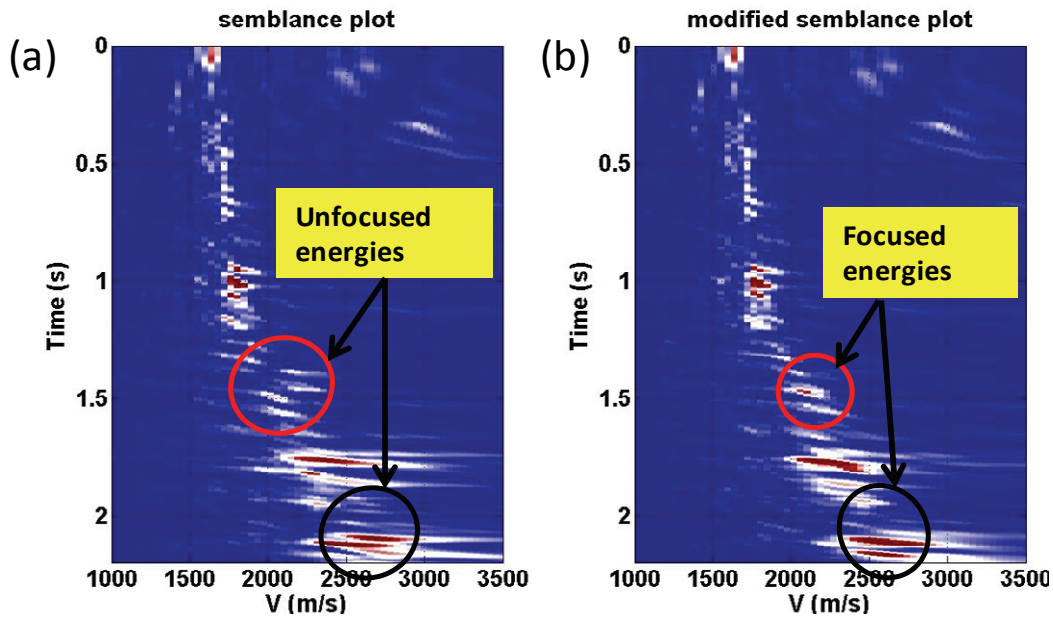


FIG. 12. Comparison of (a) regular semblance plot with (b) semblance according to linear time shift hyperbolic Radon transform with optimum α .

FUTURE WORK: INTERVAL VELOCITY INVERSION FROM MIGRATION VELOCITY

Hubral (1977) introduced the concept of the image ray (shown in Figure 14) which provides the connection between the time-migration coordinates and the regular Cartesian coordinates. Among all rays starting at a subsurface point and reaching the Earth's surface, image rays have minimal travel time. In this section we describe briefly the content of the papers Cameron (2007 and 2007a) and Cameron and Sethian (2008) regarding interval velocity estimation for time to depth conversion.

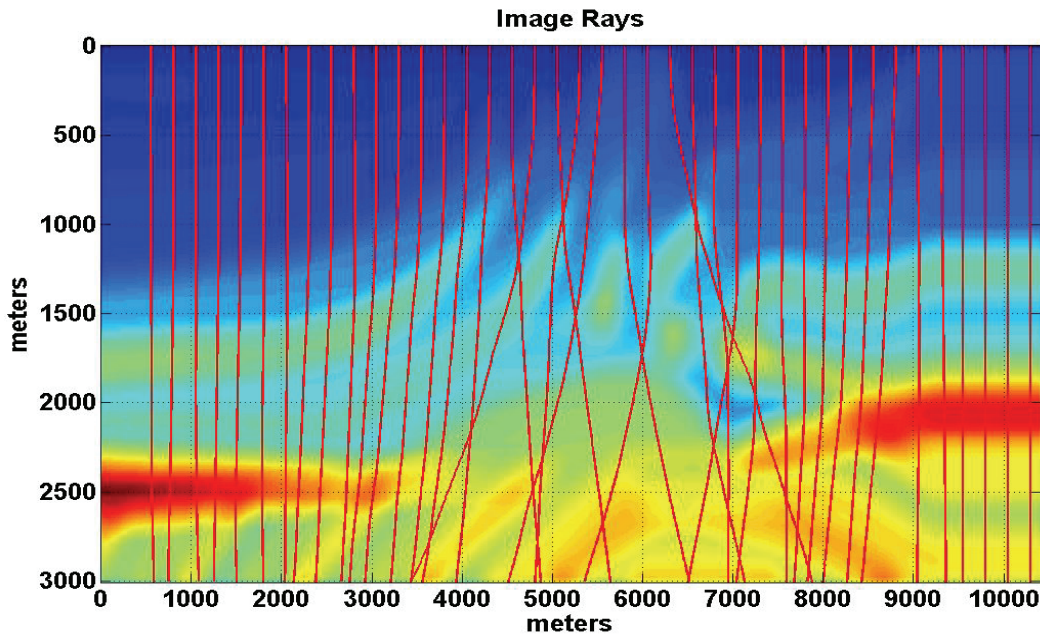


FIG. 14. Traced image rays of Marmousi model.

Conversion of the migration velocity to seismic velocity is given by

$$t_0 v_m^2(x_0, t_0) = v(x_0) R(x_0, t_0). \quad (8)$$

Here R is the reciprocal radius of curvature of the emerging wave front. Dix (1955) established the first connection between the migration velocities and the seismic velocities for the case where velocity depends only on depth. He showed that the migration velocities are the RMS velocities, if the distances between the sources and the receivers are small, the layers are plane horizontal, and the velocity is constant within each layer. For such cases, for the continuously changing velocity in $2D$ the Dix velocities are given by

$$v_{Dix}(x_0, t_0) = \left[\frac{\partial [t_0 v_m^2(x_0, t_0)]}{\partial t_0} \right]^{1/2}. \quad (9)$$

Seismic velocities and time migration velocities are connected through the quantity Q which characterizes the degree of convergence or divergence of the image rays. Q is a

scalar in $2D$ and a 2×2 matrix in $3D$. The simplest way to introduce Q is the following: take an image ray $x(x_0, t_0)$, call it central, and trace it from the surface downward into the Earth. Consider a small tube of rays around it. All these rays start perpendicular to the surface from a small neighbourhood dx_0 of the point. Thus, they represent a fragment of a plane wave propagating downward. Consider the fragment of the wave front defined by this ray tube at a time t_0 . Let dq be the fragment of the tangent to the front at the point $x(x_0, t_0)$, bounded by the ray tube. Then, in $2D$,

$$Q(x_0, t_0) = \frac{dq}{dx_0}. \quad (10)$$

In $2D$, the Dix velocities $v_{Dix}(x_0, t_0)$ which are the conventional estimate of the seismic velocities $v(x, z)$ from the time migration velocities $v_m(x_0, t_0)$ is given by

$$v_{Dix}(x_0, t_0) \equiv \left[\frac{\partial}{\partial t_0} (t_0 v_m^2(x_0, t_0)) \right]^{1/2} = \frac{v(x(x_0, t_0), z(x_0, t_0))}{|Q(x_0; t_0)|}. \quad (11)$$

Note that here t_0 is the one-way travel time along the image ray and that we denote the depth direction by z . For the case that velocity only depends on depth and the lateral velocity variation is negligible the magnitude of $|Q(x_0, t_0)|$ is close to one and the Dix inversion equation (9) is obtained.

To accomplish this, the following steps are required to be taken:

Step 1. Ray tracing algorithm which computes the image rays.

Step 2. Using the image rays found in step 1, compute the geometrical spreading which equals $\det[Q]$ (Popov 2002) and determine the velocity $v(x_0, t_0)$ from the input data. Our direction will be to study the literature on numerical solutions of elliptic PDE's to refine the results.

Step 3. Convert the velocities $v(x_0, t_0)$ given in the time coordinates (x_0, y_0, t_0) to depth and determine $v(x, y, z)$.

CONCLUSIONS

CSP gathers as an intermediate product of EOM were used for velocity analysis. In this study we simulated the behaviour of CSP gathers using ray tracing and constructing the wavefronts. We demonstrated that because of lateral velocity changes in the areas that have structurally dipping interface, the CSP data will be tilted and asymmetrical about the vertical axis. The tilt is caused by an additional linear time shift to its corresponding normal hyperbola. This causes the lack of clarity and accuracy in velocity picking in the semblance plots. We used three approaches to deal with the tilts in velocity picking. First we analysed semblance plots of left and right sided CSP gather separately and took the average velocity value. Second, we approximated the tilted hyperbola parameters by least

squares analysis and rotate its principle axis to vertical, and then found the velocity. Third, we introduced a Linear Time Shifted Hyperbolic Radon (LTSHR) transform to find the optimum value of the tilt coefficient, to remove its unfocussing effects and consequently, increasing the resolution of semblance plots.

ACKNOWLEDGMENTS

The authors would like to thank all CREWES sponsors, staff and students for their support. we also thank Gary F. Margrave, Hugh Geiger and Pat Daley for their useful suggestions and comments.

REFERENCES

- Audebert, F., Biondi, B., Lumley, D., Nichols, D., Rekdal, T., and Urdaneta, H., 1994., Marmousi travelttime computation and imaging comparisons, SEP-80, 49–69.
- Bancroft, J.C., 1996, Velocity sensitivity for equivalent offset prestack migration , Ann. Mtg: Can. Soc. Of Expl Geophys.
- Bancroft, J. C., Geiger, H. D., and Margrave, G. F., 1998, The equivalent offset method of prestack time migration: Geophysics, **63**, 2042-2053.
- Bancroft, J. C., Geiger, H. D., Foltinek, D. S., and Wang, S., 1994, Prestack migration by equivalent offsets and CSP gathers, CREWES Research Report.
- Cameron, M., Fomel, S. and Sethian, J., 2007, Seismic velocity estimation from time migration: Inverse Problems, **23**, 1329-1369.
- Cameron, M. K., 2007a, Seismic velocity estimation from time migration, Thesis, ProQuest.
- Cameron, M. and Sethian, J., 2008, Study of a Cauchy problem for a nonlinear elliptic PDE for seismic velocity estimation from time migration: Inverse Problems, submitted.
- Červený, V., 2001, Seismic Ray theory, Cambridge University Press, Cambridge.
- Claerbout, J. F., 1985, Imaging the earth interior: Blackwell scientific publications.
- Dix, C. H., 1955, Seismic velocities from surface measurements: Geophysics, **20**, 68-86.
- Fowler, J. F., 1997, A comparative overview of prestack time migration methods: 66th Ann. Internat. Mtg., Soc. Expl. Geophys., Expanded Abstracts, 1571–1574.
- Hogan, C. M. and Margrave, G. F., 2009, An interactive velocity modelling tool in MATLAB, CREWES Research Report.
- Hubral, P., 1977, Time-migration - some ray-theoretical aspects: Geophys. Prosp. **25**, 738-745.
- Hubral, P., Krey, T., 1980, Interval velocities from seismic reflection time measurements: SEG
- Leary P. O., 2004, Direct and specific least-square fitting of hyperbolæ and ellipses, Journal of Electronic Imaging **13**(3), 492– 503.
- Margrave, G.F., Bancroft, J.C. and Geiger, H.D, 2001, Fourier prestack migration by equivalent wavenumber: Geophysics, **64**, 197-207.
- Popov, M.M., 2002, Ray theory and Gaussian beam method for geophysicists, EDUFBA.
- Versteeg, R. J., 1993, Sensitivity of prestack depth migration to the velocity model: Geophysics, **58**, 873-882.
- Versteeg, R. J., 1994, The Marmousi experience: velocity model determination on a synthetic complex data set, Rice University
- Yilmaz, Ö., 1989, Velocity-stack processing: Geophys. Prosp., **37**, 357-382.